Modulation of RAS and PI3-AKT pathway by Stavudine (d4T) in PBMC of Alzheimer's Disease Patients

Francesca La Rosa (flarosa@dongnocchi.it)
Fondazione Don Carlo Gnocchi Onlus https://orcid.org/0000-0003-3181-9505
Chiara Paola Zoia
Universita degli Studi di Milano-Bicocca
Chiara Bazzini
Bicol University
Alessandra Bolognini
Universita degli Studi di Milano-Bicocca
Marina Saresella
Fondazione Don Carlo Gnocchi Onlus
Elisa Conti
Universita degli Studi di Milano-Bicocca
Carlo Ferrarese
Universita degli Studi di Milano-Bicocca
Federica Piancone
Fondazione Don Carlo Gnocchi Onlus
Ivana Marventano
Fondazione Don Carlo Gnocchi Onlus
Daniela Galimberti
Ospedale Maggiore Policlinico
Chiara Fenoglio
Ospedale Maggiore Policlinico
Elio Scarpini
Ospedale Maggiore Policlinico
Mario Clerici
Fondazione Don Carlo Gnocchi Onlus

Research

Keywords: Alzheimer's disease, Autophagy, Amyloid-β, NLRP3-inflammasome, Neuroinflammation, Stavudine (d4T).

Posted Date: August 20th, 2020

DOI: https://doi.org/10.21203/rs.3.rs-61796/v1

Abstract

Background: $A\beta_{42}$-deposition plays a pivotal role in AD-pathogenesis by inducing the activation of microglial cells and neuroinflammation. This process is antagonized by microglia-mediated clearance of Aβ plaques. Activation of the NLRP3 inflammasome is involved in neuroinflammation and in the impairments of Aβ-plaques clearance. Stavudine (d4T) on the other hand down-regulates the NLRP3 inflammasome and stimulates autophagy-mediated Aβ-clearing in a TPH-1 cell line model.

We explored the effect of d4T on Aβ-autophagy using PBMC of AD patients that were primed with LPS and stimulated with Aβ in the absence/presence of d4T. We analyzed the NLRP3 activity by measuring NLRP3-ASC complexes formation by AMNIS Flow-sight and pro-inflammatory cytokines (IL-1β, IL-18 and Caspase-1) production by ELISA. Western blot analyses were used to measure phosphorylation and protein expression of p38, CREB, ERK and AKT, p70, LAMP 2A, Beclin-1 and Bax.

Results: Data showed that d4T: 1) down regulates NLRP3 inflammasome activation and the production of down-stream proinflammatory cytokines even in PBMC; 2) stimulates the phosphorylation of AKT, ERK, p70 as well as LAMP2A production, but does modulate beclin-1, suggesting a selective effect of this compound on chaperone-mediated autophagy (CMA); 3) up regulates p-CREB and BAX, possibly diminishing Aβ-mediated cytotoxicity; and 4) reduces the phosphorylation of p-38, a protein involved in the production of pro-inflammatory cytokines.

Conclusions: d4T reduces the activation of the NLRP3 inflammasome and stimulates CMA autophagy as well as molecular mechanisms that modulate cytotoxicity and reduce inflammation in cells of AD patients. It might be interesting to verify the possibly beneficial effects of d4T in the clinical scenario.

Background

Alzheimer's disease (AD), the most prevalent type of dementia, is characterized by the deposition of amyloid-β (Aβ), the formation of neurofibrillary tangles, and neuroinflammation [1]. Thus, in AD patients Aβ accumulation induces the release of inflammatory mediators by the microglia; this facilitates Aβ deposition and neuroinflammation in a self-feeding pathogenic loop [2]. Microglia, on the other hand, plays an important role against AD that is mediated by the generation of Aβ-specific antibodies, the clearance of amyloid plaques, and the recruitment of peripheral immune cells that cross the blood-brain barrier (BBB) in an attempt to remove Aβ aggregates [3–5]. The initiation of the inflammatory response by microglia and peripheral immune cells involves cytosolic multiprotein platforms known as inflammasomes. The NLRP3 inflammasome is the best characterized of such platforms and its formation requires multiple steps. In a priming step, transcriptionally-active signalling receptors induce the NF-kB-dependent induction of NLRP3 itself, as well as that of the caspase-1 substrates pro-IL-1β and IL-18 [6]; a second signal leads to the assembly of a multimolecular complex with ASC and Caspase-1. At this point procaspase-1 or procaspase-8 are recruited [7], ASC specks are formed [8], caspases are activated, and cytokines are produced.

Activation of the NLRP3 inflammasome is a tightly regulated process; autophagy, in particular, an adaptive response to stress, down regulates NLRP3 inflammasome activation by a complex metabolic mechanism [9] that includes different molecular pathways [10–14]. Notably, autophagy defects in myeloid cells results in the aberrant activation of the inflammasome [15, 16], leading to development of inflammatory disorders. Different compounds can modulate the NLRP3 inflammasome activation as well Stavudine (d4T), a nucleoside reverse transcriptase inhibitor (NRTIs), in particular was shown to hamper NLRP3 inflammasome activation as well as caspase-1 and IL-18 production both *in vivo* [17, 18] and in a TPH-1 cell line *in vitro* model [19]. Notably, in this model d4T did not have any effect on Aβ-phagocytosis, but it stimulated autophagy-mediated Aβ-clearing [19], as witnessed by its ability to modulate the ERK1/2 and AKT pathways and to upregulate LAMP-2A and p70-S6K, their downstream targets.

Given the fact that: 1) autophagy is necessary for the degradation of Aβ in microglia; 2) p-AKT [20] and p-ERK [21] associate with Aβ-accumulation and τ-phosphorylation in AD animal models [22, 23]; and 3) autophagy is modulated by d4T [19], we explored more in details the mechanisms responsible for d4T-mediated autophagy clearing of Aβ. To this end we used peripheral blood mononuclear cells of AD patients that were stimulated with LPS + Aβ in the absence/presence of d4T.

Results

1. Patient's characteristics

Epidemiological, clinical and genetic characteristics of AD patients enrolled in the study are presented in Table 1. CSF biomarkers analysis were analyzed in all the patients and included the concentration of $A\beta_{42}$, t-t, and p-t (i.e. phosphorylated at threonine 181 or p- t 181p). Each CSF biomarker was dichotomously classified as positive or negative according to validated cut-off values: Cut-off thresholds of normality were: Aβ ≥ 600 pg/ml; t ≤500 pg/ml for individuals older than 70; Ptau ≤ 61 pg/ml [24]. Results are shown in Table 1.

2. d4T down-regulates NLRP3-complex activation and inflammasome derived cytokines

d4T was shown to significantly reduce the activation of the NLRP3 inflammasome in a THP-1-derived macrophage cell line that was LPS-primed and Ab_{42}-stimulated; we verified whether the same effect could be observed in PBMC of AD patients. Results obtained when NLRP3 and apoptosis-associated speck-like protein containing CARD (ASC)-speck formation was investigated showed that ASC speck formation was significantly increased in LPS-primed and Ab_{42}-stimulated compared to unstimulated cells ($p< 0.05$)(Fig. 1a), and indicated that ASC-speck positive cells were significantly decreased by d4T ($p< 0.05$)(Fig. 1b). d4T prevented the generation of ASC-specks, impeding the assembly of NLRP3-inflammasome complexes: the percentage of cells co-localizing ASC and NLRP3 i.e. cells in whom a fully functional NLRP3 inflammasome complex is formed, was significantly reduced ($p < 0.05$) in LPS+Ab_{42}-

stimulated cells in the presence of d4T (Fig.1c). These results were confirmed when activated Caspase-1,IL-18 and IL-1b production was analyzed. Thus, IL-1b, IL-18 and activated Caspase-1 production was significantly increased in LPS+Ab_{42} stimulated PBMC of AD patients ($p < 0.05$)(data not shown) and the production of all these proteins was reduced by d4T (Fig. 2 a,b,c); the differences reached statistically significance for IL-18 ($p = 0.004$) (Fig. 2. a) and activated caspase-1 ($p = 0.001$) (Fig. 2.b).

3. Effect of d4T on autophagy-pathways

Interaction of NLR domains with autophagy proteins provides a mechanism for direct NLR regulation of autophagy. In particular, inflammasome-forming NLRs were interact with beclin1, a pivotal protein in autophagy; we thus next investigated the ability of d4T to modulate authophagy.

Beclin-1, and phospho-p70S6K signals were examined using WB analysis in protein extract of PBMCs from AD patients that were either unstimulated (med) or LPS-primed and Ab_{42} stimulated in the absence/presence of d4T. Beclin-1, an index of the activation of p-ERK1/2- and p-AKT-mediated macro-autophagy was only marginally increased by d4T in LPS-primed and Ab_{42}-stimulated-PBMCs (Fig.3a). Phosphorylation of p70S6Kinase, their down-stream target, on the other hand, was significantly increased by d4T ($p < 0.005$). Notably, both phospho-p70S6K isoforms: the 70 KDa cytosolic form and the 85KDa nuclear one, were significantly upregulated by d4T (Fig 3b).

4. Modulation of MEK-(ERK and p38) and AKT-Protein Kinesis pathways by d4T

The NLRP3 inflammasome can also negatively regulate autophagy by reducing the expression of phosphatases and kinases. This was analyzed by evaluating ERK, p38 and AKT phosphorylation in PBMC of AD patients that were either unstimulated (med) or had been LPS-primed and Ab_{42} stimulated in the absence/presence of d4T. Results showed that all these proteins was increased in LPS+Ab_{42} stimulated PBMC. Addition of d4T to cell cultures significantly down-modulated p38 ($p = 0.0008$)(Fig 4a) whereas it further up-regulated p-ERK1,2 ($p = 0.025$)(Fig. 4b) and p-AKT ($p = 0.015$) (Fig 4c). Finally, LAMP2A, a protein in the AKT-mediated pathway that plays a pivotal role in chaperon (CMA) mediated autophagy, was significantly increased by d4T in LPS-primed and Ab_{42}-stimulated-PBMCs ($p=0.0007$) (Fig. 5).

5. Downstream MEK and AKT pathways: CREB and Bax

Protein expression of CREB and Bax, two essential downstream mediators in the ERK and AKT-mediated pathways, as well as CREB phosphorylation (p-CREB) status were analyzed next in the same cultural conditions. Also in this case, the level of these proteins was increased in LPS+Ab_{42} stimulated PBMC. d4T resulted in a further upregulation of both p-CREB ($p = 0.017$) (Fig 6a) and Bax ($p = 0.0024$) (Fig 6b).

Discussion

Microglia-driven neuroinflammation has been identified as a key player in the pathogenesis of AD; deposition of $A\beta_{42}$ in particular is an early event in the disease that induces microglia-activation and inflammation. It has been shown that this process is highly dependent on the activation of the NLRP3/ASC-inflammasome both in microglial cells [25, 26] and in circulating peripheral monocytes [27]. Thus, systemic inflammation triggers a neuroinflammatory response that results in microglial activation with deleterious consequences for learning and memory in rodent models [28–30] and in humans [31–37]. Neuroinflammation has also convincingly been shown to down regulate autophagy [38–40] we have recently described how NLRP3/ASC-inflammasome activation hampers microglial clearance of Aβ in an *in vitro* experimental model of macrophages-derived THP-1 cell line [19]. Notably, in that experimental setting Stavudine (d4T), a prototypical NRTI designed used in HIV-infection prevented active Caspase-1 release but it did not restore microglial Aβ phagocytosis. Given this background, we investigated Aβ-stimulated inflammation and autophagy and the effects of d4T on these processes using peripheral blood immune cells of AD patients.

Results herein show that d4T is capable of significantly reducing NLRP3 inflammasome activation and the down-stream production of IL-18 and Caspase-1 even in PBMC of AD patients, but had only a marginal effect on IL-1β. Recent results showed that gasdermin D, a substrate for caspases that mediates the activation of pyroptosis no NLRP3-dipendent, induces the formation of pores in the plasma membrane. Because pores can serve as a gate for the release of mature IL-1β from cells [41, 43], this could explain the different behavior of IL-18, Caspase-1 and IL-1β.

Results obtained when autophagy was analyzed showed that p-AKT- and p-ERK as well as the expression of Bax, p-CREB, LAMP2A, and of the cytosolic and nuclear p70S6 Kinase isoforms was increased in d4T-stimulated PBMC of AD patients, indicating that d4T up regulates the downstream AKT- and MEK-kinase pathways. In contrast Beclin-1 was modulated by d4T, suggesting that this compound mainly stimulates chaperone-mediated autophagy (CMA).

Autophagy is a complex molecular system that removes damaged organelles and proteins from the cytoplasm and is involved in programmed cell death and neurodegeneration; importantly, autophagy also represents an alternative pathway of cellular defense by removing intracellular pathogens [44]. The three main forms of autophagy are: macroautophagy-beclin-1 dependent, microautophagy endosomal mediated, and CMA the latter is associated with lysosomal degradation and is mediated by a cytoplasmic complex of chaperone proteins, including p70S6K, that interacts with LAMP2A [45, 46]. The phosphorylation of p70S6K by AKT signal is also able to interact with Atg proteins, promoting phagosoma formation in mTOR-independent way [47]. All these three forms of autophagy crosstalk with each other to eliminate aberrant proteins and modulating cell apoptosis [48].

Emerging evidences show that CMA is involved in the degradation of several proteins associated with neurodegenerative diseases [46] including α-synuclein [48, 50], huntingtin [51] and amyloid precursor

protein [52]. Degradation by CMA involves the selective delivery of single proteins to lysosomes upon the recognition and binding of a specific KFERQ-like pentapeptide motif to cytosolic hsp70 [53]. The chaperone-substrate complex binds the cytosolic tail of LAMP2A, triggering its assembly into a multimeric complex (protein target, KFERQ, p70S6K and LAMP2A) that mediates substrate translocation in lysosome [54, 55]. CMA is modulated by the AKT and ERK signaling pathways: p-AKT- and p-ERK; both these proteins were increased by d4T in Aβ-stimulated PBMC of AD patients, as were Bax, p-CREB, p-p70S6K and LAMP2A. Because active AKT can phosphorylate a variety of downstream molecules including Bax and CREB, these results indicate that d4T can up regulate this whole signaling pathways.

d4T-induced modulation of CREB is particularly important as this protein has a well-documented role in neuronal plasticity, and long-term memory formation, and, on the other hand, CREB alterations result in oxidative stress, apoptosis, and neurodegeneration [56]. Importantly, p-CREB expression is reduced in PBMC of AD subjects [57, 58]. d4T-induced Bax upregulation is potentially important as well, as Bax is a pro-apoptotic protein that promotes mitochondrial membrane permeabilization. d4T-mediated up regulation of p-CREB and Bax could thus stimulate CMA and apoptosis to counteract Aβ toxicity. Notably, behavioral symptoms and progression of AD in a murine model were shown to be alleviated by the activation of PI3K/AKT signaling pathway [59]. Increased p-AKT expression and activation of Bax-mediated apoptosis were also demonstrated to improve the memory capacity of AD rats [60].

Potentially important is also the effect of d4T on p38. Thus, p38 is activated in macrophages, neutrophils, and T cells by extracellular mediators of inflammation including cytokines, chemokines, and LPS [61–62], and phospho-p38 induces Th1 immune response and the production of proinflammatory cytokines [63]. The observed d4T down-regulation of this protein thus could be beneficial in reducing neuroinflammation in AD.

Conclusions

Efficient autophagic activity prevents the activation of inflammasomes [64], and stimulation of autophagy was shown to reduce soluble τ, as well as Aβ and amyloid plaques in 3xTgAD mice [65]. These results will need to be confirmed, possibly using animal models of AD. In conclusion, herein we show results obtained in peripheral immune cells of AD patients that indicate how d4T, beside reducing NLRP3 inflammasome activation, up-regulates CMA as well as CREB phosphorylation and the pro-apoptotic protein Bax. Taken together, these findings could warrant the investigation of the use of D4T the clinical scenario.

Methods

Patients

Thirteen AD patients who fulfilled inclusion criteria for a clinical diagnosis of AD were randomly selected within a large database of patients consecutively admitted between January 2017 and September 2019

by the Fondazione IRCCS Ca' Granda Ospedale Maggiore Policlinico in Milano, Italy. All patients were enrolled in a cognitive rehabilitation experimental program and underwent complete medical and neurological evaluation, laboratory analysis, CT scan or MRI, and other investigations (e.g., EEG, SPET scan, CSF examination, etc.) to exclude reversible causes of dementia. The clinical diagnosis of AD was performed according to the NINCDS-ADRDA work group criteria [66] and the DMS IV-R (American Psychiatric Association) [67]. Neuropsychological evaluation and psychometric assessment were performed with a Neuropsychological Battery that included Mini Mental State Examination (MMSE) [68].

Digit Span Forward and Backward, Logical Memory and Paired Associated Words Tests, Token Test, supra Span Corsi Block Tapping Test, Verbal Fluency Tasks, Raven Colored Matrices, the Rey Complex Figure, Clinical Dementia Rating Scale (CDR) [69]; the study conformed to the ethical principles of the Helsinki Declaration.

All patients underwent lumbar puncture (LP) for quantification of Aβ, total tau (T-t), and tau phosphorylated at position 181 (P-t) in the CSF. Normality cut-off thresholds were: Ab ≥ 600 pg/ml; t ≤ 500 pg/ml for individuals older than 70 and ≤ 450 pg/ml for individuals aged between 50 and 70 years; P-t ≤ 61 pg/ml. The Institutional Review Board of the Fondazione Cà Granda, IRCCS Ospedale Maggiore Policlinico (Milan, Italy) approved this study. All patients (or their legal guardians) gave their written informed consent for this research before entering the study.

APO e4 genotyping

Apoe genotype was determined by allelic discrimination as previously described [70]. APOE genotyping was available for all subjects and was dichotomized as being a carrier of at least one allele ε4 or carrying no ε4 allele.

CSF collection and Aβ and tau determination

CSF was collected between 8 and 10 a.m. after one-night fasting by LP in the L3/L4 or L4/L5 interspace according to standardized local procedures. CSF samples were centrifuged in 1500 rpm for 10 minutes at 4C°. The supernatants were aliquoted in polypropylene tubes and stored at -80 °C. CSF cells, glucose, and proteins were determined. CSF Aβ, tau and P tau were measured using commercially available sandwich enzyme-linked immunosorbent assay (ELISA) kits (Fujirebio, Ghent, Belgium).

Blood sample collection and processing

Whole blood was collected in vacutainer tubes containing ethylenediaminetetraacetic acid (EDTA) (Becton Dickinson & Co., Rutherford, NJ, USA). Peripheral blood mononuclear cells (PBMC) were separated on lympholyte separation medium (Cedarlane, Hornby, Ontario, CA) and washed twice in PBS

at 1500 RPM for 10 min; viable leukocytes were determined using a TC20 Automated Cell Counter (Biorad Hercules,California, USA).

d4T Cellular toxicity

Viability of PBMC incubated with d4T was determined using the MTT 3-(4,5-dimethylthiazol-2,5-diphenyltetrazolium bromide) (Sigma-Aldrich) assay, as previously described [71].

Cell cultures

PBMC were resuspended in RPMI 1640 (PAN-Biotech GmbH, Am Gewerbepark, DE) supplemented with 10% human serum, L-glutamine (2 mM), and 1% penicillin (Invitrogen, Ltd, Paisley, UK) in 6-wells plate and incubated at 37 $^{\circ}$C in a humidified 5% CO_2 atmosphere. Cells ($7x10^6$/well) were either cultured in medium alone (Medium) or were primed with Lypopolisaccaride (LPS) (1mg/ml)(Sigma-Aldrich, St. Louis, MO) for 2 hours and stimulated with Ab_{42} (10mg/ml Sigma-Aldrich, St. Louis, MO) for 22 hours in the absence/presence of d4T (50mM) (Sigma-Aldrich) [72].

Enzyme-Linked Immunosorbent Assay (ELISA)

IL-1β, IL-18, and activated Caspase-1 production was analyzed in supernatants of PBMC that were resuspendend in medium alone or were stimulated (see above) by sandwich immunoassays according to the manufacturer's instructions (Quantikine Immunoassay; R&D Systems, Minneapolis, MN, USA).

Image Stream Analysis by FlowSight AMNIS

PBMCs ($2x10^6$), stimulated as described above, were fixed with 100µl of PFA (1%) (BDH, UK), permeabilized with 100µl of Saponine (0.1%) (Life Science VWR, Lutterworth, Leicestershire, LE), and stained with FITC-anti human NLRP3 (Clone #768319, isotype Rat IgG2a, R&D Systems, Minneapolis, MN, USA) and PE-anti human ASC (clone HASC-71, isotype mouse IgG1, Biolegend, San Diego, CA, USA) for 1 h at room temperature; cells were then washed with PBS, centrifuged at 1,500 rpm for 10 min, resuspended in 50µl of PBS, and examined using the AMNIS FlowSight. Results were analyzed by IDEAS analysis software (Amnis Corporation, Seattle, WA, USA). The analysis of NLRP3 expression was performed by internalization feature utilizing a mask representing the whole cell, defined by the brightfield (BF) image, and an internal mask defined by eroding the whole cell mask. Apoptosis-associated speck-like protein containing CARD speck formation was analyzed using the same mask of internalization feature, differentiating diffuse or spot (speck) fluorescenceinside of cells. Threshold mask was used to separate all ASC positive cells population in ASC-Speck spot cells or ASC-diffuse cells by the different

diameter of the spot area: in ASC-speck, the spot shows a small area and high max pixel vice versa in cell with ASC-diffuse.

Protein extraction

Cytosol protein-extraction was performed in cultured PBMC by Cell Extraction Buffer (BioSource) containing 1mM PMSF, protease and phosphatase inhibitor cocktail (Sigma-Aldrich) (1:200 and 1:100). After incubation for 30min on ice, lysates were centrifuged at 12,000g for 10 minutes at 4°C. Protein concentration was determined by Bradford assay at 595nm.

Western Blot

Proteins (15mg) were separated by electrophoresis into 4-12% NuPAGE® Bis-Tris gels (Invitrogen) and blotted on nitrocellulose filter (GE Healthcare). Blots were blocked 1 hour at room temperature on a shaker in 5% fat-free dried milk in TBS-T buffer (50mM Tris-HCl pH 7.6, 200mM NaCl, 0.1% Tween 20). Blots were incubated over night on a shaker at 4°C with the following rabbit Antibody (Ab): anti-beclin1 (1:300, Cell Signaling), anti-LAMP2A (1:400, Abcam) anti-p-p38 (T180/Y182 1:350, Cell Signaling) anti-pERK1/2 (T202/Y204 1:300, Cell-Signaling), anti-pAKT (S473 1:500, Cell Signaling), anti-p-p70S6K (1:500 Cell Signaling), anti-pCREB (1:800, Biosource) and mouse anti-Bax (1:300, Chemicon). Abs were diluted in 5% fat-free dried milk in TBS-T buffer. A mouse anti-actin Ab (1:20000, Sigma-Aldrich) was used as internal standard. A peroxidase-linked anti-rabbit/mouse (1:5,000; Sigma-Aldrich) IgG secondary Ab was incubated for 1 hour, at room temperature on an orbital shaker in TBS-T buffer containing 3% fat-free dried milk. Signals were detected by chemiluminescent reagents (ECL Plus Kit; Amersham), visualized on X-ray film, quantified using ImageJ software and expressed as the ratio between the target and the actin signals.

Statistical analysis

Quantitative data were not normally distributed (Shapiro–Wilk test) and are thus summarized as median and interquartile range. Comparisons between the different cultural conditions were made using: 1) a 2-tailed Mann–Whitney U test performed for independent samples for NLRP3 complex, cytokines and caspases production quantified by Elisa; 2) One-way repeated ANOVA test, followed by Tukey's multiple comparison test for protein extracts evaluated by WB analysis. Data analysis was performed using the MedCalc statistical package (MedCalc Software bvba, Mariakerke Belgium). *p*-Values of less than 0.05 were considered statistically significant.

Abbreviations

Ab =amyloid beta

AD =Alzheimer’s Disease

AKT = protein kinase b;

ASC =apoptosis-associated speck-like protein containing card

Bax = bcl-2-like protein 4,

BBB = blood-brain barrier

CMA = chaperone autophagy mediated

CSF= cerebrospinal fluid

CREB= camp response element-binding protein

d4T = stavudine

ELISA = enzyme-linked immunosorbent assay

ERK= extracellular signal-regulated kinases

IL-1b = interleukin 1-beta

IL-18 = interleukin-18

LAMP2a = lysosome-associated membrane protein 2

LPS: lipopolysaccaride

NLRP3 = nod-like receptor 3

PBMC = peripheral blood mononuclear cells

t = Tau

WB = western blotting

Declarations

Ethics approval and consent to participate

The study was conducted in accordance with the Helsinki Declaration. Informed consent was obtained from the patients. Informed consent to participate in this study was given by allsubjects or their caregivers. All samples were obtained from the Neurodegenerative Disease Unit of the Fondazione Cà Granda,IRCCS Ospedale Maggiore Policlinico, University of Milan (Milan,Italy)

Consent for publication

Not applicable.

Availability of data and materials

The datasets used and/or analysed during the current study are available from the corresponding author on reasonable request.

Competing interests

The authors declared no potential conflicts of interest with respect to the research, authorship, and/or publication of this article.

Funding

This research was supported by 2018-2019 Ricerca Corrente, Italian Ministry of Health.

Authors’ contributions

FLR, CPZ, MS and MC conceived and designed the experiments. CB, AB, EC, FP, IM performed the experiments and analyzed the data. FLR and CPZ wrote the paper, and MC revised it. CF, DG, ES and CF are responsible for the clinical cohorts of patients. All authors read and approved the final paper.

Acknowledgments

The authors thank all the subjects enrolled in the study.

References

1. Haass C, Selkoe DJ. Soluble protein oligomers in neurodegeneration: lessons from the Alzheimer's amyloid beta-peptide. Nat Rev Mol Cell Biol. 2007. doi:10.1038/nrm2101.
2. Cai Z, Hussain MD, Yan LJ. Microglia, neuroinflammation, and beta-amyloid protein in Alzheimer's disease. Int Neurosc. 2014. doi:10.3109/00207454.2013.833510.
3. Heneka MT. Macrophages derived from infiltrating monocytes mediate autoimmune myelin destruction. J Exp Med. 2014. doi:10.1084/jem.2118insight1.
4. Zhang F, Jiang L. Neuroinflammation in Alzheimer’s disease. Neuropsychiatr Dis Treat. 2015. doi:10.2147/NDT.S75546.

5. Van Dyck CH. Anti-Amyloid-β Monoclonal Antibodies for Alzheimer's Disease: Pitfalls and Promise. Biol Psychiatry. 2018. doi:10.1016/j.biopsych.2017.08.010.
6. Agostini L, Martinon F, Burns K, McDermott MF, Hawkins PN, Tschopp J. NALP3 forms an IL-1beta-processing inflammasome with increased activity in Muckle-Wells autoinflammatory disorder. Immunity. 2004. doi:10.1016/s1074-7613(04)00046-9.
7. Sagulenko V, Thygesen SJ, Sester DP, Idris A, Cridland JA, Vajjhala PR, Roberts TL, Schroder K, Vince JE, Hill JM, et al. AIM2 and NLRP3 inflammasomes activate both apoptotic and pyroptotic death pathways via ASC. Cell Death Differ. 2013. doi:10.1038/cdd.2013.37.
8. Masumoto J, Taniguchi S, Ayukawa K, Sarvotham H, Kishino T, Niikawa N, Hidaka E, Katsuyama T, Higuchi T, Sagara J. ASC, a novel 22-kDa protein, aggregates during apoptosis of human promyelocytic leukemia HL-60 cells. J Biol Chem. 1999; 26;274(48):33835-8.
9. Nakahira K, Haspel JA, Rathinam VA, Lee SJ, Dolinay T, Lam HC, Englert JA, Rabinovitch M, Cernadas M, Kim HP, et al. Autophagy proteins regulate innate immune responses by inhibiting the release of mitochondrial DNA mediated by the NALP3 inflammasome. Nat Immunol. 2011. doi:10.1038/ni.1980.
10. Kiffin R, Christian C, Knecht E, Cuervo AM. Activation of chaperone-mediated autophagy during oxidative stress. Mol Biol Cell. 2011. doi:10.1091/mbc.e04-06-0477.
11. Martinez-Lopez N, Athonvarangkul D, Mishall P, Sahu S, Singh R. Autophagy protein regulate ERK phosphorylation. Nat Commun. 2013. doi:10.1038/ncomms3799.
12. Harris J, Lang T, Thomas JPW, Sukkar MB, Nabar NR, Kehrl JH. Autophagy and inflammasomes. Mol Immunol. 2017. doi:10.1016/j.molimm.2017.02.013.
13. Yu L, Chen Y. Autophagy pathway: Cellular and molecular mechanisms. Autophagy. 2018. doi:10.1080/15548627.2017.1378838.
14. Shibutani ST, Saitoh T, Nowag H, Münz C, Yoshimori T. Autophagy and autophagy-related proteins in the immune system. Nat Immunol. 2015. doi:10.1038/ni.3273.
15. Hara T, Nakamura K, Matsui M, Yamamoto A, Nakahara Y, Suzuki-Migishima R, Yokoyama M, Mishima K, Saito I, Okano H, et al. Suppression of basal autophagy in neural cells causes neurodegenerative disease in mice. Nature. 2006. doi:10.1038/nature04724.
16. Jessop F, Hamilton RF, Rhoderick JF, Shaw PK, Holian A. Autophagy deficiency in macrophages enhances NLRP3 inflammasome activity and chronic lung disease following silica exposure. Toxicol Appl Pharmacol. 2016. doi:10.1016/j.taap.2016.08.029.
17. Fowler BJ, Gelfand BD, Kim Y, Kerur N, Tarallo V, Hiran, Amarnath S, Fowler DH, Radwan M, Young MT. Nucleoside reverse transcriptase inhibitors possess intrinsic anti-inflammatory activity. Science. 2014. doi:10.1126/science.1261754.
18. Cai R, Liu L, Luo B, Wang J, Shen J, Shen Y, Zhang R, Chen J, Lu H. Caspase-1 Activity in CD4 T Cells Is Downregulated Following Antiretroviral Therapy for HIV-1 Infection. AIDS Res Hum Retroviruses. 2017. doi:10.1089/AID.2016.0234.

19. La Rosa F, Saresella M, Marventano I, Piancone F, Ripamonti E, Al-Daghri N, Bazzini C, Zoia CP, Conti E, Ferrarese C, et al. Stavudine Reduces NLRP3 Inflammasome Activation and Modulates Amyloid-β Autophagy. J Alzheimers Dis. 2019. doi:10.3233/JAD-181259.
20. Kirouac L, Rajic AJ, Cribbs DH, Padmanabhan J. Activation of Ras-ERK Signaling and GSK-3 by Amyloid Precursor Protein and Amyloid Beta Facilitates Neurodegeneration in Alzheimer's Disease. eNeuro. 2017. doi:10.1523/ENEURO.0149-16.2017.
21. Heras-Sandoval D, Ferrera P, Arias C. Amyloid-β protein modulates insulin signaling in presynaptic terminals. Neurochem Res. 2012;37(9):1879–85. doi:10.1007/s11064-012-0800-7.
22. Lin MW, Chen YH, Yang HB, Lin CC, Hung SY. Galantamine Inhibits $A\beta_{1-42}$-Induced Neurotoxicity by Enhancing α7nAChR Expression as a Cargo Carrier for LC3 Binding and $A\beta_{1-42}$ Engulfment During Autophagic Degradation. Neurotherapeutics. 2019. doi:10.1007/s13311-019-00803-7.
23. Wang X, Wang Y, Zhu Y, Yan L, Zhao L. Ther.Neuroprotective Effect of S-trans, Trans-farnesylthiosalicylic Acid via Inhibition of RAS/ERK Pathway for the Treatment of Alzheimer's Disease. Drug Des Devel Ther. 2019. doi:10.2147/DDDT.S233283.
24. Sjögren M, Vanderstichele H, Agren H, Zachrisson O, Edsbagge M, Wikkelsø C, Skoog I, Wallin A, Wahlund LO, Marcusson J. Tau and Abeta42 in cerebrospinal fluid from healthy adults 21–93 years of age: establishment of reference values. Clin Chem. 2001;47(10):1776–81.
25. Halle A, Hornung V, Petzold GC, Stewart CR, Monks BG, Reinheckel T, Fitzgerald KA, Latz E, Moore KJ, Golenbock DT. The NALP3 inflammasome is involved in the innate immune response to amyloid-beta. Nat Immunol. 2008. doi:10.1038/ni.1636.
26. Heneka MT, Kummer MP, Stutz A, Delekate A, Schwartz S, Vieira-Saecker A, Griep A, Axt D, Remus A, Tzeng TC, et al. NLRP3 is activated in Alzheimer's disease and contributes to pathology in APP/PS1 mice. Nature. 2013. doi:10.1038/nature11729.
27. Saresella M, La Rosa F, Piancone F, Zoppis M, Marventano I, Calabrese E, Rainone V, Nemni R, Mancuso R, Clerici M. The NLRP3 and NLRP1 inflammasomes are activated in Alzheimer's disease. Mol Neurodegener. 2016. doi:10.1186/s13024-016-0088.
28. Semmler A, Okulla T, Sastre M, Dumitrescu-Ozimek L, Heneka MT. Systemic inflammation induces apoptosis with variable vulnerability of different brain regions. J Chem Neuroanat. 2005. doi:10.1016/j.jchemneu.2005.07.003.
29. Semmler A, Frisch C, Debeir T, Ramanathan M, Okulla T, Klockgether T, Heneka MT. Long-term cognitive impairment, neuronal loss and reduced cortical cholinergic innervation after recovery from sepsis in a rodent model. Exp Neurol. 2017. doi:10.1016/j.expneurol.2007.01.003.
30. Weberpals M, Hermes M, Hermann S, Kummer MP, Terwel D, Semmler A, Berger M, Schäfers M, Heneka MT. NOS2 gene deficiency protects from sepsis-induced long-term cognitive deficits. J Neurosci. 2009. doi:10.1523/JNEUROSCI.3238-09.2009.
31. Qin L, Wu X, Block ML, Liu Y, Breese GR, Hong J, Knapp DJ, Crews FT. Systemic LPS causes chronic neuroinflammation and progressive neurodegeneration. Glia. 2007. doi:10.1002/glia.20467.

32. Semmler A, Hermann S, Mormann F, Weberpals M, Paxian SA, Okulla T, Schäfers M, Kummer MP, Klockgether T, Heneka MT. Sepsis causes neuroinflammation and concomitant decrease of cerebral metabolism. J Neuroinflammation. 2008. doi:10.1186/1742-2094-5-38.
33. Semmler A, Widmann CN, Okulla T, Urbach H, Kaiser M, Widman G, Mormann F, Weide J, Fliessbach K, Hoeft A, et al. Persistent cognitive impairment, hippocampal atrophy and EEG changes in sepsis survivors. J Neurol Neurosurg Psychiatry. 2013. doi:10.1136/jnnp-2012-302883.
34. Iwashyna TJ, Ely EW, Smith DM, Langa KM. Long-term cognitive impairment and functional disability among survivors of severe sepsis. JAMA. 2010. doi:10.1001/jama.2010.1553.
35. Gyoneva S, Swanger SA, Zhang J, Weinshenker D, Traynelis SF. Altered motility of plaque-associated microglia in a model of Alzheimer's disease. Neuroscience. 2016. doi:10.1002/glia.22686.
36. Widmann CN, Heneka MT. Long-term cerebral consequences of sepsis. Lancet Neurol. 2014. doi:10.1016/S1474-4422(14)70017-1.
37. Tejera D, Mercan D, Sanchez-Caro JM, Hanan M, Greenberg D, Soreq H, Latz E, Golenbock D, Heneka MT. Systemic inflammation impairs microglial Aβ clearance through NLRP3 inflammasome. Embo J. 2019. doi:10.15252/embj.2018101064.
38. Fésüs L, Demény Ma, Petrovski G. Autophagy shapes inflammation. Antioxidants & redox signaling. 2011; doi.org/10.1089/ars.2010.3485.
39. Erivan SRJ, Morandini AC, Gasdermin: A new player to the inflammasome game. Biomedical Journal Volume 40, Issue 6, 2017; doi.org/10.1016/j.bj.2017.10.002.
40. Shi J, Gao W, Shao F Pyroptosis: gasdermin-mediated programmed necrotic cell death. Trends Biochem Sci. 2017;42:245e54.
41. Deretic V, Levine B. Autophagy balances inflammation in innate immunity. Autophagy. 2018;14(2):243–51.
42. Netea-Maier RT, Plantinga TS, Van De Veerdonk FL, Smit JW, Netea MG. Modulation of inflammation by autophagy: consequences for human disease. Autophagy. 2016; doi:10.1080/15548627.2015.1071759.
43. Mizushima N, Levine B, Cuervo AM, Klionsky DJ. Autophagy fights disease through cellular self-digestion. Nature. 2008; doi:10.1038/nature06639.
44. Bejarano E, Cuervo AM. Chaperone-Mediated Autophagy. Proc Am Thorac Soc. 2010; doi:10.1513/pats.200909-102JS.
45. Kaushik S, Cuervo A. Chaperone-mediated autophagy: a unique way to enter the lysosome world. Trends Cell Biol. 2012; doi: 10.1016/j.tcb.2012.05.006.
46. Klionsky DJ,Meijer AJ,Codogno P, Neufeld TP, Scott RC. Autophagy and p70S6 Kinase. Autophagy.2015; doi.org/10.4161/auto.1.1.1536.
47. Ferrucci M, Biagioni F, Ryskalin L, Limanaqi F, Gambardella S, Frati A, Fornai F. Ambiguous Effects of Autophagy Activation Following Hypoperfusion/Ischemia. Int J Mol Sci. 2018; doi:10.3390/ijms19092756.

48. Soto C. Unfolding the role of protein misfolding in neurodegenerative diseases. Nature Rev Neurosci. 2003; doi:10.1038/nrn1007.
49. Cuervo AM, Stefanis L, Fredenburg R, Lansbury PT, Sulzer D. Impaired degradation of mutant α-synuclein by chaperone-mediated autophagy. Science. 2004; doi:10.1126/science.1101738.
50. Vogiatzi T, Xilouri M, Vekrellis K, Stefanis LWild type alpha-synuclein is degraded by chaperone-mediated autophagy and macroautophagy in neuronal cells. J Biol Chem. 2008; doi:10.1074/jbc.M801992200.
51. Qi L, Zhang XD, Wu JC, Lin F, Wang J, DiFiglia M, Qin ZH. The role of chaperone–mediated autophagy in huntingtin degradation. PLoS One. 2012; doi: 10.1371/journal.pone.0046834.
52. Tai HC, Serrano-Pozo A, Hashimoto T, Frosch MP, Spires-Jones TL, Hyman BT. The synaptic accumulation of hyperphosphorylated tau oligomers in Alzheimer disease is associated with dysfunction of the ubiquitin-proteasome system. Am J Pathol. 2012; doi: 10.1016/j.ajpath.2012.06.033.
53. Ciechanover A, Kwon YT. Degradation of misfolded proteins in neurodegenerative diseases: therapeutic targets and strategies. Exp Mol Med. 2015; doi: 10.1038/emm.2014.117.
54. Kiffin R, Christian C, Knecht E, Cuervo AM. Activation of chaperone-mediated autophagy during oxidative stress. Mol Biol Cell. 2004; doi:10.1091/mbc.e04-06-0477.
55. Kaushik S, Massey AC, Mizushima N, Cuervo AM. Constitutive activation of chaperone-mediated autophagy in cells with impaired macroautophagy. Mol Biol Cell. 2008. doi:10.1091/mbc.E07-11-1155.
56. Mayr B, Montminy M. Transcriptional regulation by the phosphorylation-dependent factor CREB. Nat Rev Mol Cell Biol. 2008. doi:10.1038/35085068.
57. Carlezon WA, Duman RS, Nestler EJ. The many faces of CREB. Trends Neurosci. 2005. doi:10.1016/j.tins.2005.06.005.
58. Bartolotti N, Bennett DA, Lazarov O. Reduced pCREB in Alzheimer's disease prefrontal cortex is reflected in peripheral blood mononuclear cells. Molecular Psychiatry. 2016; doi.org/10.1038/mp.2016.111.
59. Li H, Kang T, Qi B, Kong L, Jiao Y, Cao Y, Zhang J, Yang J. Neuroprotective effects of ginseng protein on PI3K/Akt signaling pathway in the hippocampus of d-galactose/AlCl3 inducing rats model of Alzheimer's disease. J. Ethnopharmacol. 2016; doi: 10.1016/j.jep.2015.12.020.
60. Zhang B, Wang Y, Li H, Xiong R, Zhao Z, Chu X, Li Q, Sun S, Chen S. Neuroprotective effects of salidroside through PI3K/Akt pathway activation in Alzheimer's disease models. Drug Des. Dev. Ther. 2016; doi: 10.2147/DDDT.S99958.
61. Singh RK, Diwan M, Dastidar SG, Najmi AK. Differential effect of p38 and MK2 kinase inhibitors on the inflammatory and toxicity biomarkers in vitro. Hum Exp Toxicol. 2018; doi: 10.1177/0960327117715901.
62. Ronkina N, Menon MB, Schwermann J. Map kap kinases Mk2 and Mk3 in inflammation: complex regulation of tnf biosynthesis via expression and phosphorylation of tristetraprolin. Biochem

pharmacol. 2010; doi: 10.1016/j.bcp.2010.06.021.
63. Gaestel M, Kotlyarov A, Kracht M. Targeting innate immunity protein kinase signalling in inflammation. Nat rev drug discov. 2009; doi: 10.1038/nrd2829.
64. Abdelaziz DH, Khalil H, Cormet-Boyaka E, Amer AO. The cooperation between the autophagy machinery and the inflammasome to implement an appropriate innate immune response: do they regulate each other? Immunol Rev. 2015. doi: 10.1111/imr.12288.
65. Majumder S, Richardson A, Strong R, Oddo S. Inducing autophagy by rapamycin before, but not after, the formation of plaques and tangles ameliorates cognitive deficits. PLoS One. 2016. doi: 10.1371/journal.pone.0025416.
66. McKhann G, Drachman D, Folstein M, Katzman R, Price D, Stadlan EM. Clinical diagnosis of Alzheimer's Disease: report of the NINCDS-ADRDA Work Group under the auspices of Department of Health and Human Service Task Force on Alzheimer's Disease. Neurology 1984 34: 939–944.
67. American Psychiatric Association. Diagnostic and statistical manual of mental disorders DSM-IV-R.1994.
68. Folstein MF, Folstein SE, McHugh PR. Mini-mental state. A practical method for grading the cognitive state of patients for the clinicians. J Psychiat Res. 1975. DOI 10.1016/0022-3956(75)90026-6.
69. Hughes CP, Berg L, Danziger WL, Coben LA, Martin RL. A new clinical scale for staging of dementia. Br J Psychiatry. 1982. DOI 10.1192/bjp.140.6.566.
70. Koch W, Ehrenhaft A, Griesser K, Pfeufer A, ̈uller M, Schomig J. A., Taqman systems for geno-typing of disease-related polymorphisms present in the gene encoding Apolipoprotein E. Clin Chem Lab. 2002. DOI 10.1515/CCLM.2002.197.
71. Mosmann T. Rapid colorimetric assay for cellular growth and survival: application to proliferation and cytotoxicity assays. *J Immunol Methods.* 1983 DOI 10.1016/0022-1759(83)90303-4.
72. Gray LR, Turville SG, HItchen TL, Cheng WJ, Ellett AM, Salimi H, Roche MJ, et al. HIV-1 Entry and Trans-Infection of Astrocytes Involves CD81 Vesicles. *PLoS One* 2014 DOI 10.1371/journal.pone.0090620.

Table

Due to technical limitations, table 1 is only available as a download in the Supplemental Files section.

Figures

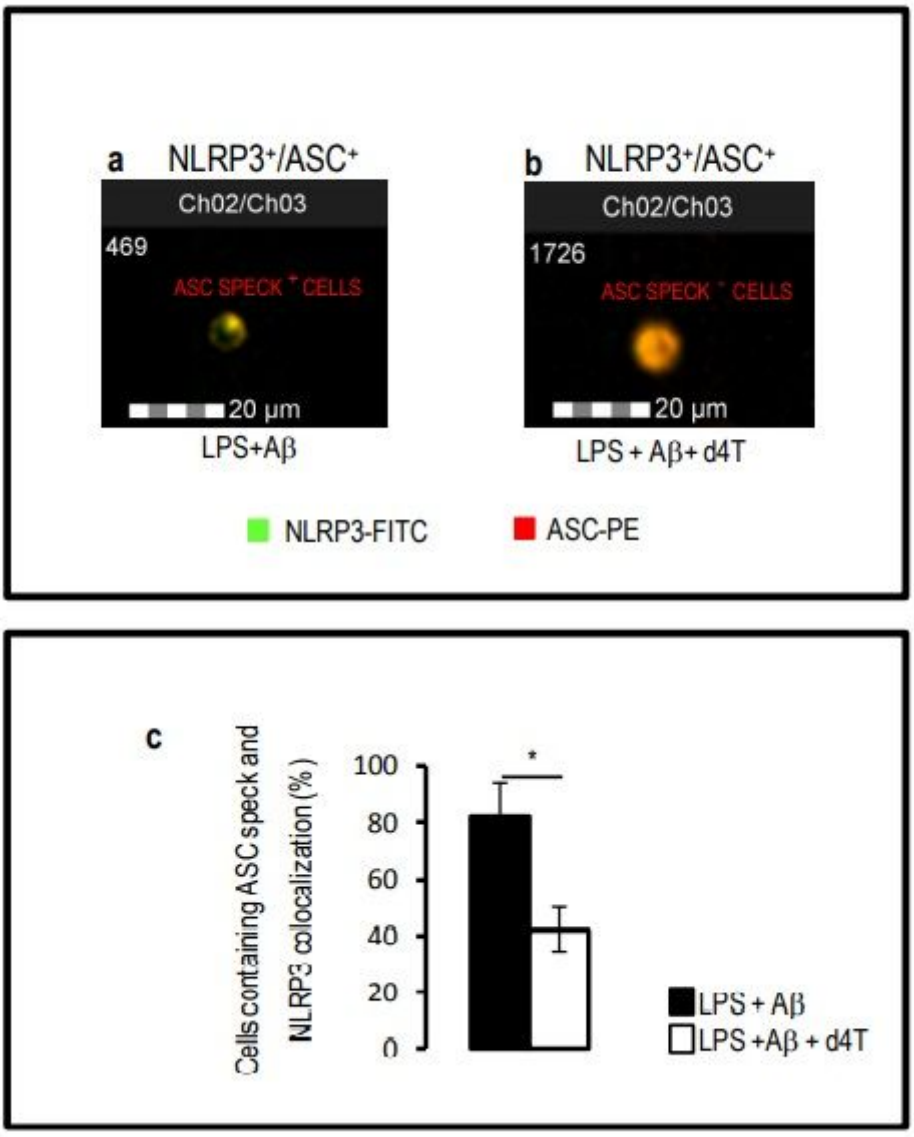

Figure 1

Inflammasome production and ASC-Speck formation. Images from a single representative experiment of Nod-like receptor protein 3 (NLRP3) expression and apoptosis-associated speck-like protein containing CARD (ASC)-speck formation in LPS-primed and A□-stimulated PBMCs of 13 AD patients in the presence/absence of d4T. ASC-speck (a) and ASC-diffuse (b) images were obtained by AMNIS FlowSight-merged (Ch02/03) NLRP3-FITC (Ch02) and ASC-PE (Ch03) fluorescences; analysis of ASC-specks and its co-localization with NLRP3 were performed by IDEAS software that provides tools to evaluate image regions (masks) and perform calculations (features). The percentage of ASC speck positive cells is shown in panel c. The statistical analysis were performed; significance was calculated by t-test (unpared) and was shown (*p <0.05).

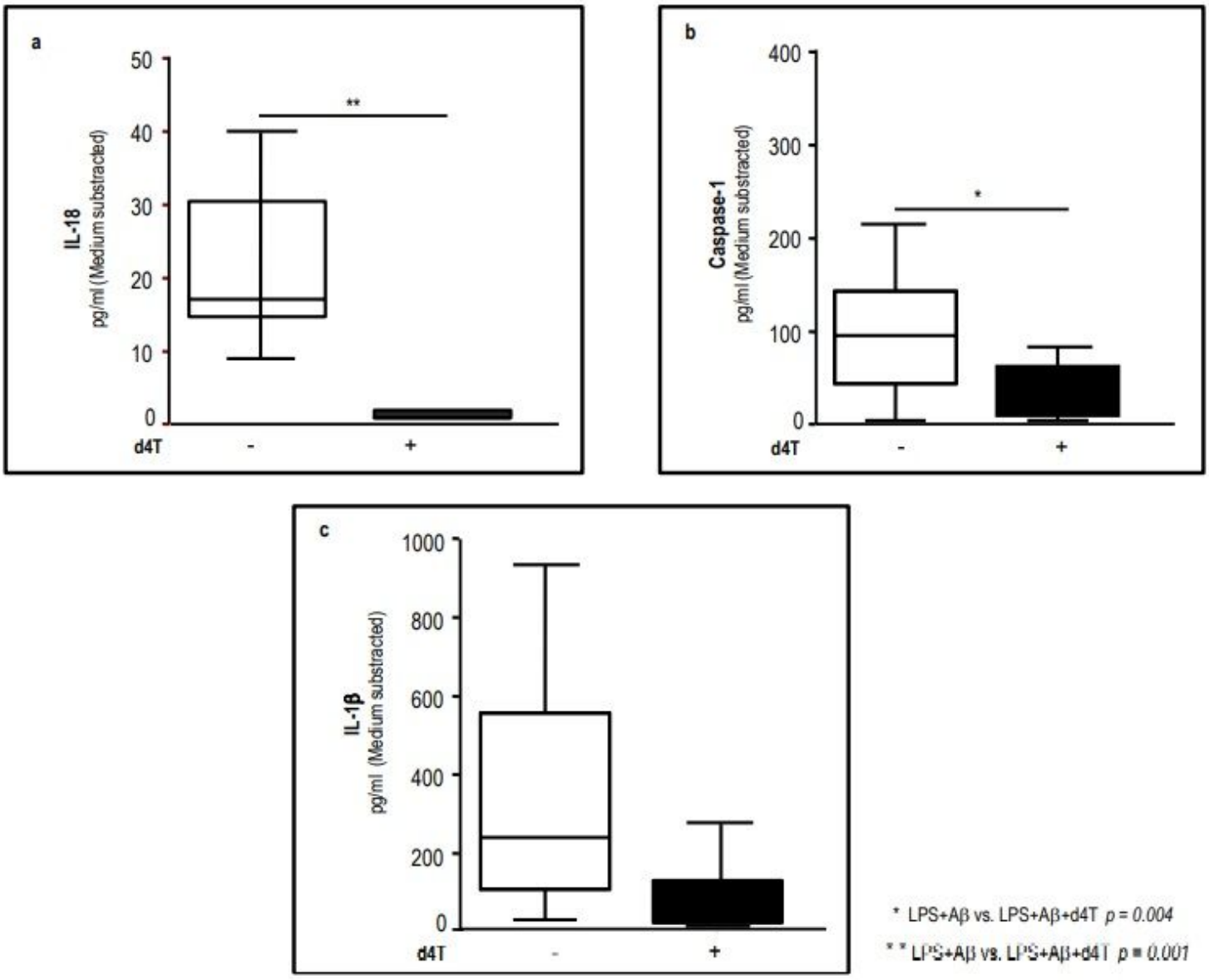

Figure 2

Caspase-1 and inflammasome effector cytokines production. IL-18 (a), Caspase-1 (b) and IL-1 (c) production by unstimulated (medium) or by LPS+A-stimulated PBMCs of 13 AD patients in the presence/absence of d4T. Data are expressed as median of cytokines and caspase-1 concentration (pg/ml) of stimulated cells medium subtracted. The statistical analysis were performed; significance was calculated by t-test (unpared) and was shown (*p <0.05).

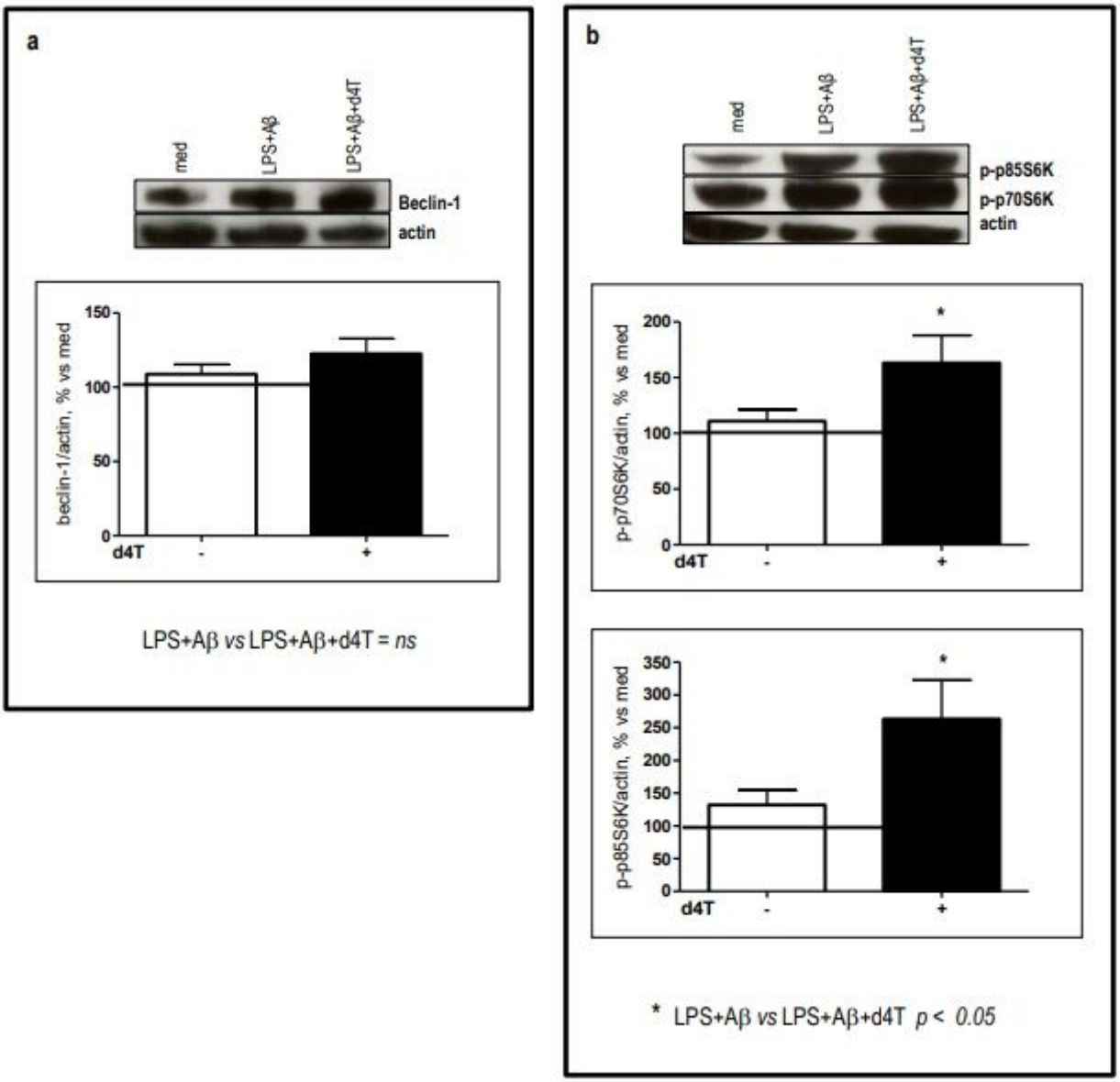

Figure 3

Beclin-1 and down-stream CMA-mediated autophagy protein production. The determination by WB of Beclin-1 (a, 52KDa) and downstream targets that are involved in CMA-autophagy as phospho-p70S6K, phospho-p85S6K (b, 70 and 85 KDa) cytosol protein extracts of LPS-primed and A□-Stimulated-PBMCs from 13 AD patients in presence/absence of Stavudine (d4T). Each result is expressed as the percentage of the ratio between phosphorylated-kinase and actin versus unstimulated cells (medium, 100%, = black line). The values are expressed as percentage means±SD. Statistical significance is shown (**p<0.001, *p<0.05). Relative representative blots from single independent experiment are shown in upper part of panels a and b Actin protein was used as a loading control (42KDa).

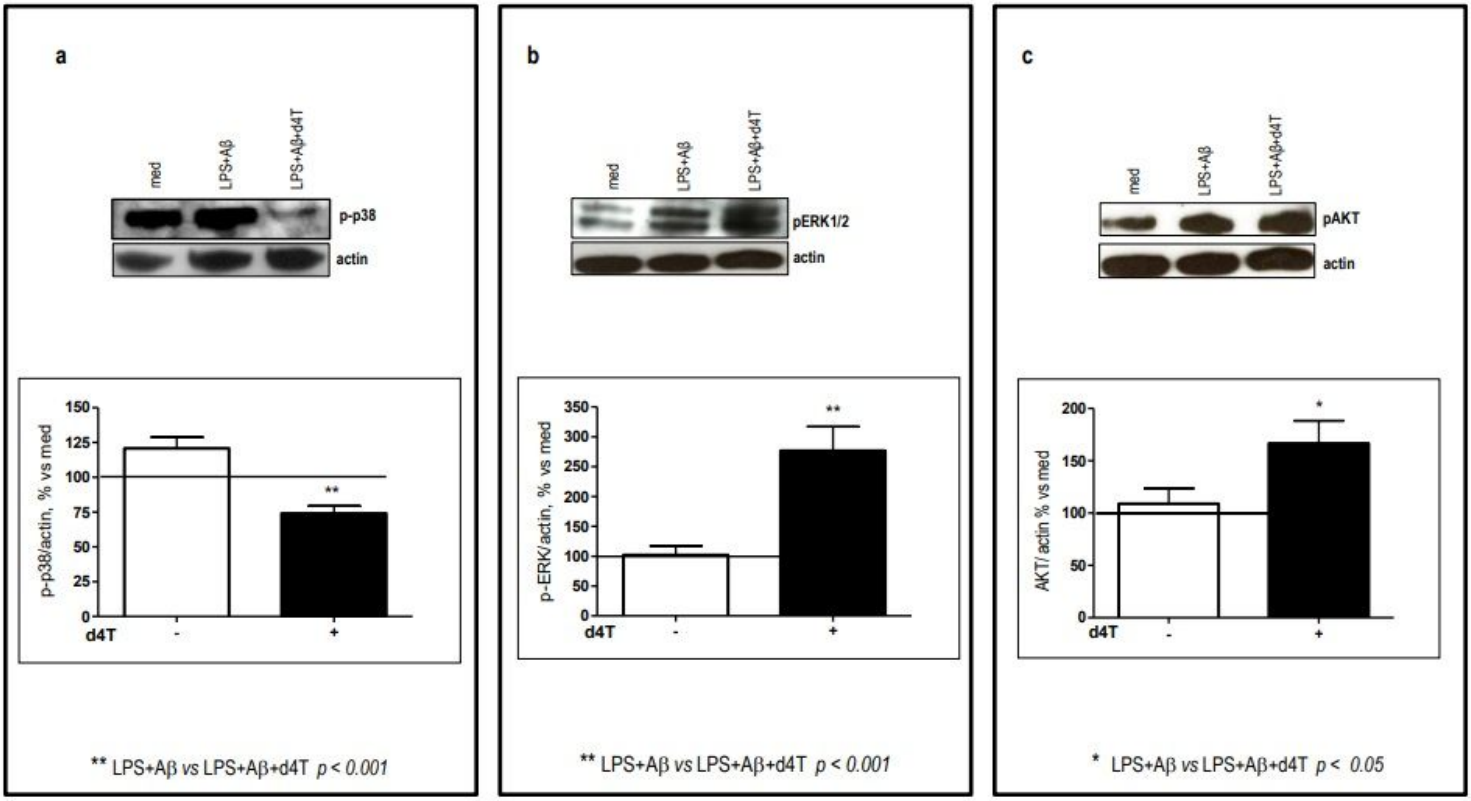

Figure 4

p-38, ERK1/2 and AKT phosphorylation. Western blot analysis (WB) of MEK-(ERK and p38) and AKT-Protein Kinesis pathways in LPS-primed and A□-stimulated-PBMCs of AD patients in the presence/absence of d4T. Phosphorylation status of p38 (38KDa)(a), ERK1/2 (42-44 KDa) (b) and AKT (60KDa) (c) kinases was evaluated in cytosol protein extracts of cells. Each result is expressed as the percentage of the ratio between phosphorylated-kinase and actin versus unstimulated cells (medium, 100%, = black line). The values are expressed as percentage means±SD. Statistical significance is shown (**p<0.001, *p<0.05). Relative representative blots from single independent experiment are shown in upper part of panels a, b, and c. Actin protein was used as a loading control (42KDa).

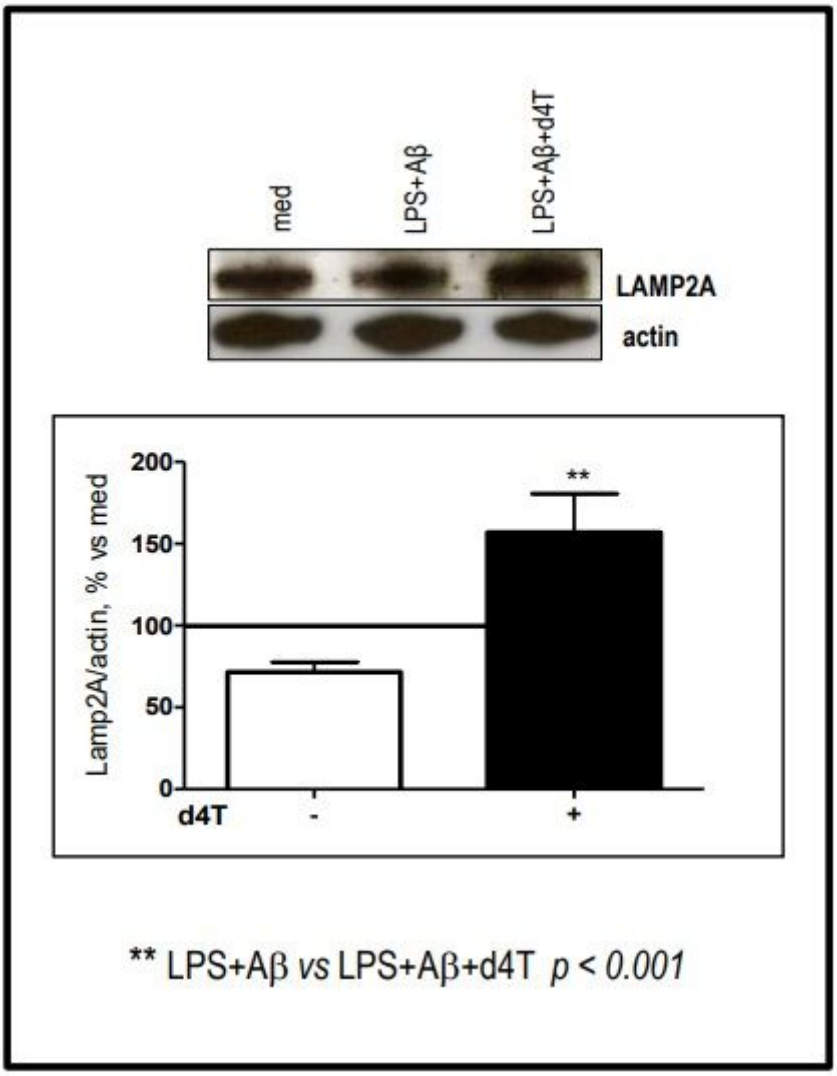

Figure 5

ERK1/2 and AKT pathways downstream target.Western blot analysis (WB) of LAMP2A (100KDa) in cytosol protein extracts of LPS-primed and A□-stimulated-PBMCs of 13 AD patients in the presence/absence of d4T. Results are expressed as the percentage of the ratio between phosphorylated-kinase and actin versus unstimulated cells (medium, 100%, = black line). The values are expressed as percentage means±SD. Statistical significance is shown (**p<0.001). Relative representative blots from single independent experiment are shown in upper part of figure. Actin protein was used as a loading control (42KDa).

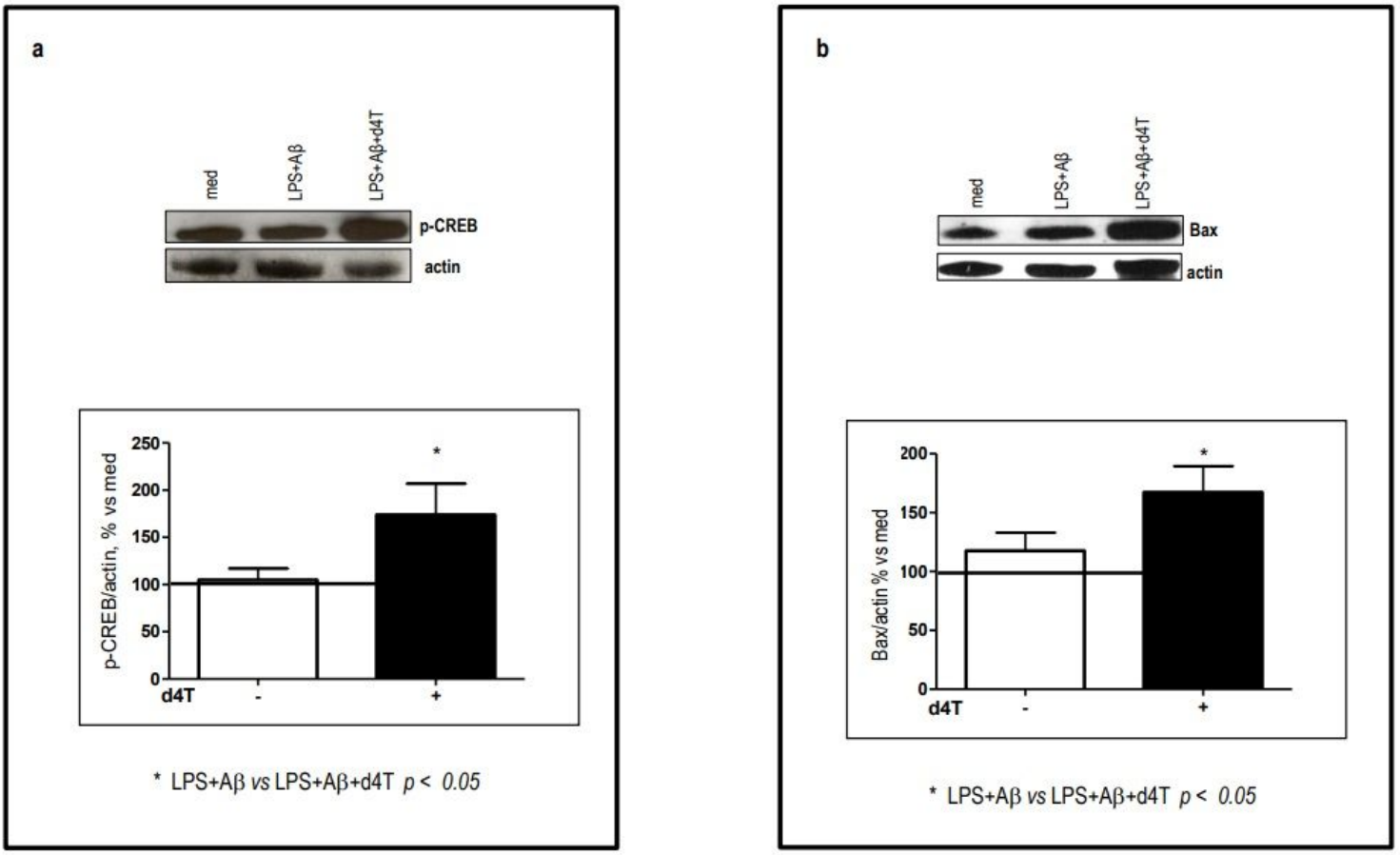

Figure 6

CREB and Bax protein production. WB analysis of the phosphorylation status of CREB (43 KDa) (a) and Bax (21KDa) (b) production in cytosol protein extracts of LPS-Primed and A-Stimulated-PBMCs from 13 AD patients in presence/absence of Stavudine (d4T). Each result is expressed as the percentage of the ratio between phosphorylated-kinase and actin versus unstimulated cells (medium, 100%, = black line). The values are expressed as percentage means±SD. Statistical significance is shown (*p<0.05). Relative representative blots from single independent experiment are shown in upper part of panels a and b. Actin protein was used as a loading control (42KDa).

Supplementary Files

This is a list of supplementary files associated with this preprint. Click to download.

- Table1.pdf